

Article

The Influence of the Hydrogen Pressure on Kinetics of the Canola Oil Hydrogenation on Industrial Nickel Catalyst

Marcin Konkol ^{*}, Waldemar Wróbel, Robert Bicki and Andrzej Gołębiowski

New Chemical Syntheses Institute, Al. Tysiąclecia Państwa Polskiego 13A, Puławy 24-110, Poland;
waldemar.wrobel@ins.pulawy.pl (W.W.); robert.bicki@ins.pulawy.pl (R.B.);
andrzej.golebiowski@ins.pulawy.pl (A.G.)

* Correspondence: marcin.konkol@ins.pulawy.pl; Tel.: +48-8-1473-1749

Academic Editor: Keith Hohn

Received: 16 February 2016; Accepted: 28 March 2016; Published: 7 April 2016

Abstract: Canola oil was hydrogenated on an industrial nickel catalyst at 180 °C under a wide range of pressures from 1.5 to 21 bar(a). The effect of hydrogen pressure on the hydrogenation characteristics and fatty acids profile was investigated. The hydrogenation kinetics were described by a simplified three-step model including linolenic acid. The apparent rate constants for the particular reaction steps (hydrogenation, isomerization) k_x as well as rate constants k_{x0} and reaction orders in hydrogen were determined. The results reveal that with the increasing pressure an increase of values of all rate constants was observed, with the largest increase being observed for the rate constant of hydrogenation of monoenes to stearic acid (about 20 times). Moreover, with the increasing pressure the isomerization rate of *cis* dienes to *trans* dienes was found to become lower than the dienes hydrogenation rate. Analogously, the *cis/trans* monoenes isomerization rate was also found to decrease with the increasing pressure. The reaction orders of the hydrogenation steps with respect to hydrogen were in the range of 0.35 to 1.1. The kinetic model was verified by comparison of predicted fatty acids contents with the experimental data of fatty acids profiles. It emerged that a simplified kinetic model proposed can be utilized to simulate the course of the hydrogenation process and concentrations of fatty acids at a certain iodine value.

Keywords: oil hydrogenation; nickel catalyst; fatty acids profile; kinetics; hydrogen pressure

1. Introduction

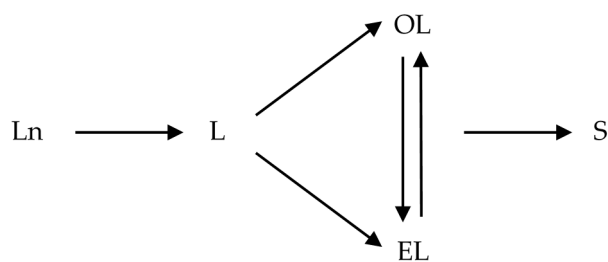
Catalytic hydrogenation/hardening of vegetable oils is one of the most important processes in the food industry. The main aim of this process is to increase the oxidative and thermal stability of edible oils and to improve their consumption suitability in the manufacture of margarines and other fats. It is estimated that the amount of oils hydrogenated every year is approximately 6 million tons [1]. Particularly important is the hydrogenation of vegetable oils which account for about 70% of edible oil in the world [2]. A typical vegetable oil consists of different triglycerides (triacylglycerols) which are the esters of glycerol and fatty acids. The chemistry and the mechanism of triglycerides partial hydrogenation process are very complex due to the fact that several reactions are likely to occur: (a) saturation of double bonds, (b) *cis/trans* isomerization of double bonds, or (c) a shift of double bonds in the carbon chain. The rate at which various chains of fatty acids are hydrogenated depends on the number of double bonds. The situation is additionally complicated by the fact that there is a high chance of different combinations of fatty acids and glycerol which, along with the possibility of hydrogenation or isomerization of only some double bonds, may lead to the formation of at least 4000 different triglycerides [3]. What is more, double bonds may undergo hydrogenation or isomerization at different rates depending on their position in the carbon chain.

There are many factors affecting the course of hydrogenation, such as type and quality of oil, temperature, hydrogen pressure, catalyst type, catalyst loading, and stirring rate [4]. The effects of these process parameters on the activity and selectivity, especially towards *trans* fatty acids (TFA) formation have been widely reported [2,5–8]. There have also been many attempts of modelling the nickel-catalyzed hydrogenation process of triacylglycerols in the literature and many investigators have determined the overall reaction rate during hydrogenation [9–14]. The first and simplest kinetic model of edible oil hydrogenation, developed in 1949 by Bailey [15], was based on three consecutive reactions of unsaturated fatty acids as presented in Scheme 1.



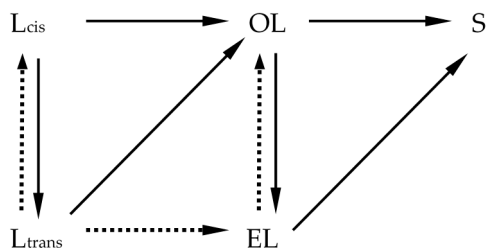
Scheme 1. Simple hydrogenation model: Ln, L, OL, EL, S denote linolenic acid, linoleic acid, oleic acid, elaidic acid, and stearic acid, respectively.

Based on further studies, it was revealed that the rates of hydrogenation for this mechanism were pseudo first-order in triglycerides [16–19]. The mechanism presented in Scheme 1 was later modified by incorporating the *cis/trans* isomerization of monoenes (Scheme 2) [20–22]. Gut *et al.* proposed a kinetic model that took into account the formation of *cis* and *trans* monoenes during hydrogenation of sunflower oil [20]. The reaction rates of the fatty acids were determined using a Langmuir-Hinshelwood adsorption kinetic equation. Their model assumed that both *cis* and *trans* fatty acids were adsorbed on the catalyst surface in the same way and that the adsorbed double bond could undergo isomerization at the catalyst surface [20]. Similarly, Fillion *et al.* investigated the kinetics of soybean oil hydrogenation using two models to describe the hydrogenation process based on Langmuir-Hinshelwood kinetic approach [10]. The preliminary simple model, based on Scheme 1, was utilized to identify the appropriate kinetic rate equations. In the second model, the *cis/trans* isomerization was taken into account as illustrated in Scheme 2.

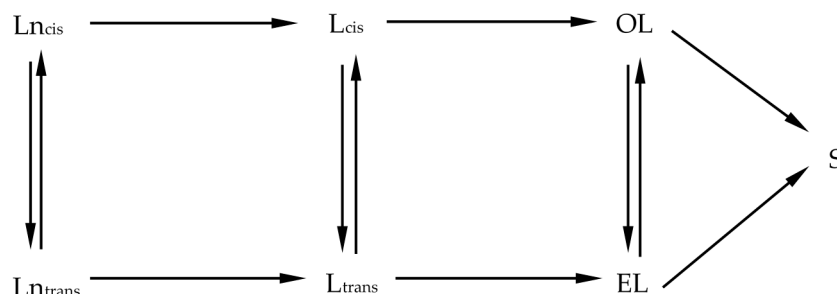


Scheme 2. Hydrogenation model with *cis/trans* isomerization of monoenes.

Plourde *et al.* studied the hydrogenation of sunflower oil on nickel catalysts in comparison with palladium catalysts supported on silica [23]. The hydrogenation process was described by a lumped kinetic model shown in Scheme 3. The rate constants for each step were determined. A dashed line indicate the reactions that can be neglected. The calculation results based on experimental data indicate that the *cis/trans* isomerization reaction of linoleic and oleic acid is practically irreversible. Furthermore, hydrogenation of *trans* C18:2 isomers to *trans* C18:1 ones was found to be negligible for a nickel catalyst. Jovanović *et al.* investigated the hydrogenation of soybean oil under industrial working conditions [24]. They used a complicated model shown in Scheme 4. An iterative procedure, incorporating numerical simulation at each step, was used to calculate rate constants of the proposed model. The results revealed that for *cis/trans* isomerization reactions the rate constants are comparably small except for the rate constant for the isomerization of oleic acid to elaidic acid. Only recently Chang *et al.* proposed a model where linolenic acid is excluded and the hydrogenation reaction of oleic acid positional isomers, 9c-C18:1 and 12c-C18:1 proceeds independently via two different pathways [25].



Scheme 3. Reaction paths for the hydrogenation of sunflower oil by Plourde *et al.* [23].



Scheme 4. Reaction paths for the hydrogenation of soybean oil by Jovanović *et al.* [24].

In the literature data, there have been few reports on the effect of the hydrogen pressure on oil hydrogenation kinetics [26,27]. Holser *et al.* performed kinetic studies of the soybean oil hydrogenation in a wide pressure range, however, the reported experimental data are very sparse [26]. The authors used a complex model to describe the hydrogenation process taking into account triglycerides profile. In some experiments the hydrogen concentration was lower than the one in equilibrium. This circumstance required taking into consideration the kinetics of hydrogen dissolving process that made the model even more complicated.

The objective of our study was to determine the effect of the hydrogen pressure on the kinetics of canola oil hydrogenation. We report the evaluation of canola oil hydrogenation carried out with a commercial nickel catalyst and the hydrogenation kinetics described by a simplified three-step model including linolenic acid. Furthermore, the influence of the hydrogen pressure on the selectivity and fatty acids (FA) profile at a given iodine value ranging from 95 to 70 has also been discussed.

2. Results and Discussion

2.1. Physicochemical Properties of the Precursor

The precursor (INS Ni) is, chemically, a mixture of nickel-aluminum hydroxycarbonates with a general formula: $\text{Ni}_m\text{Al}_n(\text{CO}_3)_x(\text{OH})_y \times z\text{H}_2\text{O}$. The physicochemical properties of the precursor, such as specific surface area (S_{BET}), pore volume (V_C), mesopore volume (V_{mes}), average pore diameter (d_{av}), nickel surface area (S_{Ni}), and nickel dispersion (D) are summarized in Table 1. The particle size of the precursor was in the range of 3 to 5 μm . The pore distribution analysis is shown in Figure 1. The pore distribution analysis revealed pores in the range of 10 to 100 nm. This corresponds to the intermediate structure between meso- and macroporous.

Table 1. Physicochemical properties of the precursor.

	S_{BET} , m^2/g	V_C , cm^3/g	V_{mes} , cm^3/g	$S_{\text{Ni-A}}$, $\text{m}^2/\text{g}_{\text{cat}}$	$S_{\text{Ni-B}}$, $\text{m}^2/\text{g}_{\text{Ni}}$	d_{av} , nm	D , %
INS Ni	70	0.34	0.17	42.6	63.1	22	9.5

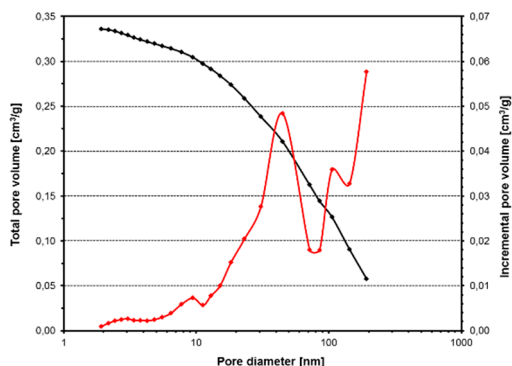
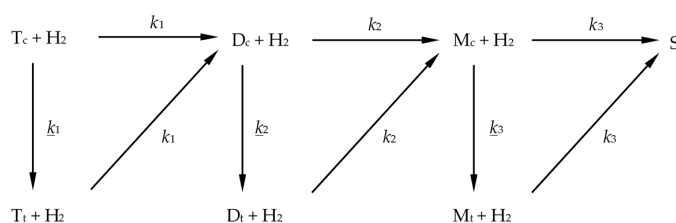


Figure 1. Pore size distribution analysis for the INS Ni precursor.

2.2. Kinetic Model

Based on the literature reports, the reaction network shown in Scheme 5 was proposed.



Scheme 5. Reaction paths for the canola oil hydrogenation ($T = C18:3$, $D = C18:2$, $M = C18:1$, $S = C18:0$).

The overall hydrogenation pathway involves the consecutive saturation of *cis* C18:3 to *cis* C18:2, *cis* C18:2 to *cis* C18:1, and *cis* C18:1 to C18:0, as well as the parallel irreversible isomerization of *cis* forms to *trans* ones. The reaction pathway may also involve the partial saturation of *trans* C18:3 to *cis* C18:2, *trans* C18:2 to *cis* C18:1, and hydrogenation of *trans* C18:1 to C18:0. The *trans* C18:3, C18:2, and C18:1 notations include all of the positional and geometrical isomers of linolenic, linoleic, and oleic acids, respectively. Such an approach to simplify the complex reaction network has also been used by other researchers [10,23]. Moreover, several other assumptions were made: (a) at each hydrogenation stage a *cis* form may isomerize to a *trans* form in an irreversible manner; (b) at each step both forms of a fatty acid react with hydrogen with the same reaction rate constant leading to a *cis* unsaturated fatty acid or saturated stearic acid in the last step; and (c) all reactions were considered to follow pseudo first-order kinetics with respect to fatty acids. Furthermore, under experimental conditions used in this work, hydrogen remained in a large excess so that its concentration was constant during the hydrogenation process and this concentration is embedded in the rate constant k .

The assumption that all reactions are the first order in fatty acids provides a possibility to express the reaction rate r for all reactions considered with an equation $r = k \times c$, where c is a molar concentration of the corresponding fatty acid. Since fatty acids are liquids and hydrogen is supplied as gas, it can be assumed that the volume of the liquid phase remains constant through the hydrogenation process. The number of moles of fatty acids also remains constant according to the Scheme 5. Therefore, since the measurements of the particular fatty acids are performed in a known reaction volume and in the presence of a known amount of a catalyst, the molar concentration c can reasonably be replaced by the number of moles of fatty acids n in the reaction system.

Taking into account the abovementioned assumptions, the rates of reactions shown in Scheme 5 can be expressed by means of a set of differential Equations (1a–f), where m is a Ni concentration in the oil:

$$\frac{1}{m} \frac{dn_{Tc}}{dt} = -k_1 \cdot n_{Tc} - \underline{k}_1 \cdot n_{Tc} \quad (1a)$$

$$\frac{1}{m} \frac{dn_{Tt}}{dt} = -k_1 \cdot n_{Tt} + \underline{k}_1 \cdot n_{Tc} \quad (1b)$$

$$\frac{1}{m} \frac{dn_{Dc}}{dt} = -k_2 \cdot n_{Dc} - \underline{k}_2 \cdot n_{Dc} + k_1 \cdot (n_{Tc} + n_{Tt}) \quad (1c)$$

$$\frac{1}{m} \frac{dn_{Dt}}{dt} = -k_2 \cdot n_{Dt} + \underline{k}_2 \cdot n_{Dc} \quad (1d)$$

$$\frac{1}{m} \frac{dn_{Mc}}{dt} = -k_3 \cdot n_{Mc} - \underline{k}_3 \cdot n_{Mc} + k_2 \cdot (n_{Dc} + n_{Dt}) \quad (1e)$$

$$\frac{1}{m} \frac{dn_{Mt}}{dt} = -k_3 \cdot n_{Mt} + \underline{k}_3 \cdot n_{Mc} \quad (1f)$$

In the case of studies of the hydrogenation process yielding the fatty acids profiles after various time intervals, the formulas being a solution of this set of differential equations can be used to determine the rate constants for a particular reaction step.

2.3. Effect of Hydrogen Pressure on Kinetics of the Canola Oil Hydrogenation

Canola oil was hydrogenated in a batch reactor using an industrial nickel catalyst denoted as INS Ni_C, containing 5.64 wt% Ni. The reactions were performed at 180 °C in a wide range of hydrogen pressures of 1.5 to 21 bar(a). This range corresponds to pressures used in the oil industry for hydrogenation of triglycerides and free fatty acids. It was verified that the agitation rate above 950 rpm had no effect on the hydrogenation rate. This indicates that above the agitation rate of 950 rpm there are no diffusional resistances for a transfer of dissolved hydrogen to the bulk liquid phase and then to the catalyst surface. Moreover, it is known that only nickel located in pores having a diameter of at least 2 nm participates in the hydrogenation reaction [7]. The pore distribution analysis of the INS Ni precursor revealed pores with a diameter of 10–100 nm and the average pore diameter was *ca.* 20 nm. According to the literature data [23,28], hampering of the hydrogenation reaction by the diffusion of reactants into the catalyst pores is low for medium-pore and wide-pore catalysts, especially with a diameter of over 4 nm (approx. twice the dimension of triglycerides).

The nickel concentration for each catalytic run was equal to 0.03 wt%. The depth of hydrogenation was controlled by measurement of the iodine value. The iodine value (IV) of an oil or a fatty acid is the mass of iodine in grams that is consumed by 100 grams of the oil/fatty acid. For all tests the hydrogenation depth of canola oil was comparable, as indicated by similar changes of iodine value (monitored by changes of refractive index) and the final iodine value of the hydrogenated canola oil of *ca.* 69–71 (determined by Wijs method). Such depth of hydrogenation corresponds to that in the production of fatty acids components for margarine and shortenings on an industrial scale. The results of the hydrogenation tests are compiled in Table 2. Two approaches for the estimation of the hydrogenation activity were used. In the first one, the activity is expressed by the hydrogen consumption per 1 g of Ni per min. The second approach is based on the overall reaction constant k_r , according to [23]. It is well-known that the saturation of double bonds follows first-order kinetics with respect to the iodine value drop as shown in Equation (2):

$$\frac{1}{m} \frac{d(IV)_t}{dt} = -k_r \cdot (IV)_t \quad (2)$$

The integration of Equation (2) using the initial conditions that $(IV)_t = (IV)_0$ at $t = 0$ gives:

$$m \cdot k_r = \frac{1}{t} \cdot \ln \left(\frac{IV_0}{IV_t} \right) \quad (3)$$

It is known that the increase of pressure causes a linear growth of hydrogen solubility in accordance with Henry's Law and, thus, it causes the increase of hydrogen concentration on the catalyst surface. This results in higher hydrogenation rates and lower amounts of *trans* isomers and other positional isomers. Wisniak and Albright measured the solubility of hydrogen in cottonseed oil

at pressures of 6.8–100 atm and temperatures in the range 50–140 °C and reported that the solubility increased with increased temperature and that Henry's Law was satisfied up to *ca.* 35 atm [12]. Moreover, Andersson *et al.* reported that the solubility of hydrogen in cottonseed oil was nearly independent of the iodine value of the oil, that means independent of a hydrogenation degree [29]. The effect of pressure on the solubility of hydrogen in canola oil was calculated according to [29] and is presented in Figure 2.

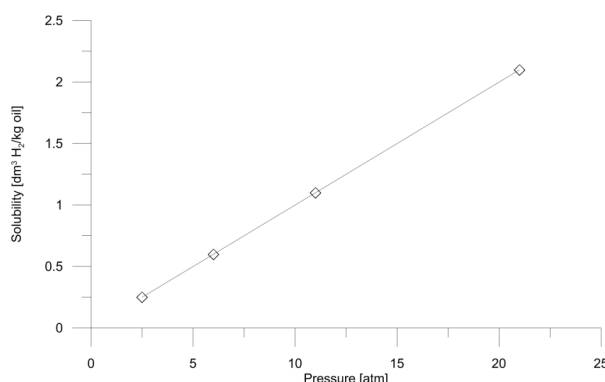


Figure 2. Relationship between pressure and hydrogen solubility (180 °C).

In line with expectations, the increase of the hydrogenation activity of the INS Ni_C catalyst was observed with increasing hydrogen pressure. The reaction time required for a decrease of iodine value by *ca.* 46–47 units (this corresponds to the hydrogen consumption of *ca.* 1000 cm³) decreased from 39 min for 2.5 bar(a) to 7 min for 21 bar(a). A 5.5-fold increase of the activity was found for two analogous hydrogenation reactions carried out under 2.5 and 21 bar(a). The hydrogenated canola oil samples with iodine value of *ca.* 70 were analyzed by means of chromatography for the profile of fatty acids. The contents of monoenes, dienes, trienes, and saturated fatty acids are presented in Table 3.

Table 2. Hydrogenation of canola oil on INS Ni_C catalyst.

Test	Pressure, bar(a)	Time, min	Activity, cm ³ H ₂ /(g Ni × min)	Change of iodine value, ΔIV	Iodine value, IV _{Wijs} ¹	mk _r , min ⁻¹	k _r , (kg of oil) × (g of Ni) ⁻¹ × min ⁻¹
1	2.5	39	3350	46.2	71.2	0.0127	0.0423
2	6	19.3	6770	46.2	-	0.0257	0.0857
3	11	12	11000	45.8	-	0.0408	0.136
4	21	7	19050	47.0	69.2	0.0724	0.241

¹ Iodine value determined by Wijs method.

Table 3. Fatty acids content (%) in samples of canola oil hydrogenated on INS Ni_C catalyst (IV~70).

Fatty acid	Non-hydrogenated canola oil	Hydrogenated canola oil			
		2.5 bar(a)	6 bar(a)	11 bar(a)	21 bar(a)
C18:0 (S)	1.7	13.1	16.3	16.7	22.1
C18:1 ^{trans} (M _t)	0	36.1	30.6	25.1	22.7
C18:1 ^{cis} (M _c)	63.2	41.2	42.6	46.1	41.8
C18:2 ^{cis} (D _c)	19.3	0.6	1.2	2.4	3.3
C18:2 ^{trans} (D _t)	0	1.5	1.8	2.0	1.9
C18:3 ^{cis} (T _c)	8.3	0	0	0.2	0.5
C18:3 ^{trans} (T _t)	0	0	0	0	0
Other	7.5	7.5	7.5	7.5	7.5

The chromatographic analysis results revealed that in the hydrogenated samples (iodine value ~70) the content of elaidic acid, 9t-C18:1, and other positional isomers decreased from 36.1 to 22.7 wt%

with the increasing pressure from 2.5 to 21 bar(a). A concurrent increase of the stearic acid content from 13.1 to 22.1 wt% was also observed. Furthermore, some deterioration of the linolenic selectivity was observed at elevated hydrogen pressures as evidenced by an increase of the *cis* C18:3 content from 0 to 0.5 wt%. Similar observations were reported by List *et al.* for the supported nickel catalyst in the soybean oil hydrogenation at various pressures [27].

The experimental data of the FA contents in hydrogenated samples of canola oil were used to determine the apparent rate constants k_x of the particular hydrogenation steps depending on the hydrogen pressure. The results are summarized in Table 4. Since no *trans* isomers of linolenic acid in hydrogenated samples were found by means of the chromatographic analysis, the \underline{k}_1 constant for isomerization of *cis* C18:3 to *trans* C18:3 could be neglected as equal to 0.

Table 4. Effect of pressure on the apparent reaction rate constants, k_x .

Pressure, bar(a)	$k_x, (\text{kg of oil}) \times (\text{g of Ni})^{-1} \times \text{min}^{-1}$				
	k_1	k_2	\underline{k}_2	k_3	\underline{k}_3
1.5	0.469	0.174	0.107	0.0072	0.044
2.5	0.575	0.236	0.126	0.013	0.061
6	0.814	0.425	0.188	0.035	0.107
11	1.04	0.562	0.212	0.059	0.138
21	1.34	0.889	0.281	0.147	0.238

It is known that the rates at which various chains of fatty acids are hydrogenated depend on the number of double bonds. The situation is additionally complicated by the fact that only some double bonds may undergo hydrogenation or isomerization and at different rates depending on the position in the carbon chain. The presented results provide a quantitative measure of the influence of hydrogen pressure on hydrogenation rates of particular reaction steps. The results reveal that, under the pressure of 1.5 bar(a), trienes are hydrogenated more than 2.5 times faster than dienes, and over 65 times faster than monoenes to stearic acid ($k_1 \sim 2.5 \times k_2 \sim 65 \times k_3$). The increase of values of all apparent rate constants was observed with the increased pressure, with the largest increase being observed for the k_3 constant of hydrogenation of monoenes to stearic acid (about 20 times). As a consequence, under 21 bar(a) the following relations of rate constants were obtained: $k_1 \sim 1.5 \times k_2 \sim 9 \times k_3$, showing a distinct increase of the monoenes hydrogenation rate. Furthermore, in case of dienes, the *cis* to *trans* isomerisation rate increased ca. 2.5 times with the increased pressure. However, this increase of the *cis/trans* isomerization rate of dienes was lower than the corresponding increase of the dienes hydrogenation rate (1.5 bar(a), $k_2/\underline{k}_2 = 1.6$; 21 bar(a), $k_2/\underline{k}_2 = 3.2$). This means that higher hydrogen pressure facilitates hydrogenation to a larger extent than *cis/trans* isomerization. Similarly, the *cis/trans* monoenes isomerization rate was also found to decrease with the increased pressure, the \underline{k}_3/k_3 ratio changed from 6.1 to 1.6 under 21 bar(a). This observation can be rationalized on the basis of the Horiuti-Polanyi mechanism [30]. According to this mechanism, the hydrogenation proceeds in two stages through a partially-hydrogenated transition state, in which only one hydrogen atom is bound. Thus, a high concentration of hydrogen on nickel surface favors hydrogenation of the partially-hydrogenated transition state at the expense of isomerization and decreases the contact time of the adsorbed molecule on the catalyst surface. The addition of the second hydrogen atom (saturation) becomes more likely than cleavage of the already bound hydrogen atom that may lead to positional or geometric isomers.

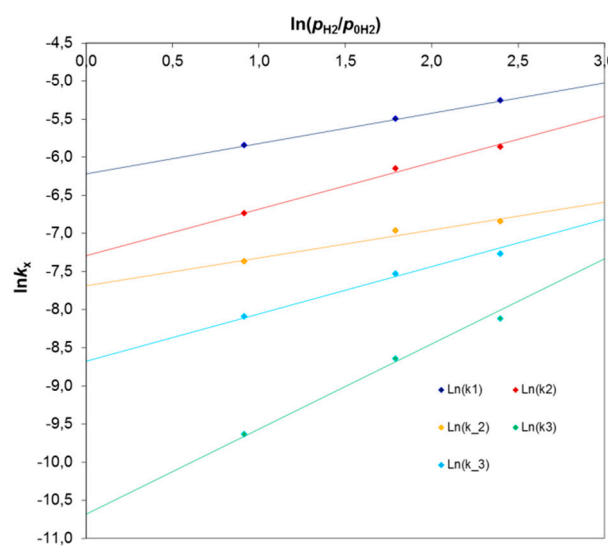
The rate constants at atmospheric pressure (k_{x0}) were determined from the following formula: $k_x = k_{x0} \times (p_{\text{H}_2}/p_{0\text{H}_2})^n$. The linear formula has a form: $\ln(k_x) = n \ln(p_{\text{H}_2}/p_{0\text{H}_2}) + \ln(k_{x0})$ where $p_{0\text{H}_2} = 1 \text{ bar (a)}$. A dependence of $\ln k_x$ from $\ln(p_{\text{H}_2}/p_{0\text{H}_2})$ for the particular apparent rate constants is presented in Figure 3. The slope of the line gives the n exponent, whereas the intercept point provides $\ln(k_{x0})$ values that are compiled in Table 5.

Table 5. Values of k_{x0} constants for $p_{0H_2} = 1$ bar(a) and n exponent.

Parameter	k_1	k_2	\underline{k}_2	k_3	\underline{k}_3
n	0.397	0.611	0.365	1.12	0.62
k_{x0}	0.399	0.136	0.092	0.0046	0.034

In all cases, very good values of R^2 coefficients in the range of 0.98–1.00 were obtained. The reaction orders (n exponent) with respect to hydrogen were in the range of 0.35 to 1.1. These values are consistent with literature reports indicating that the rates of dienes to monoenes hydrogenation and the *cis/trans* monoenes isomerization are half order with respect to the hydrogen concentration [9], while the hydrogenation reaction of monoenes follows first-order kinetics [9]. Other authors [31] arrive at the first order in hydrogen for dienes and an order of 3/2 for monoenes when hydrogenating in the gas phase.

The lumped kinetic model was verified by comparison of predicted fatty acid contents with the experimental data of FA profiles obtained for pressures 1.5 and 6 bar(a). The experimental points cover the iodine value range from 95 to 70, which is typically of interest during industrial hydrogenation of vegetable oils in order to obtain fatty acids components for the manufacture of margarine and shortenings. The results of predicted profiles of fatty acids (solid lines) along with those obtained experimentally are shown in Figures 4 and 5. As can be seen, a reasonably good consistency was found between the experimental and predicted fatty acid contents from the proposed kinetic model. The observed deviations in the course of the hydrogenation reaction between the calculated model and measured experimental points for M-*cis* (C18:1*cis*) fraction result from measurement errors (deviations in FA analysis by means of GC-MS) and simplifications assumed during the process modelling. The first pair of rate constants k_1 and \underline{k}_1 is a result of the analytical solution, whereas calculation of other pairs can be done only via numerical iterations. A character of the solved equations allows for determination of rate constants with an accuracy resulting only from constraints of floating-point calculations.

**Figure 3.** Linear relationship between $\ln k_x$ and $\ln(p_{H_2}/p_{0H_2})$; $p_{0H_2} = 1$ bar (a).

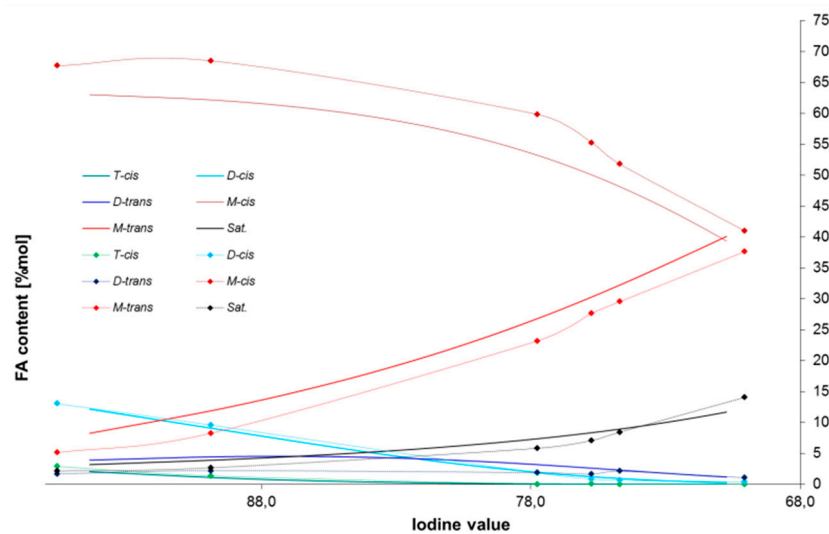


Figure 4. Predicted (solid line) and experimental (dotted line) fatty acids contents of canola oil hydrogenated with INS Ni_C catalyst. Reaction conditions: temperature 180 °C, H₂ pressure = 1.5 bar(a), agitation 950 rpm.

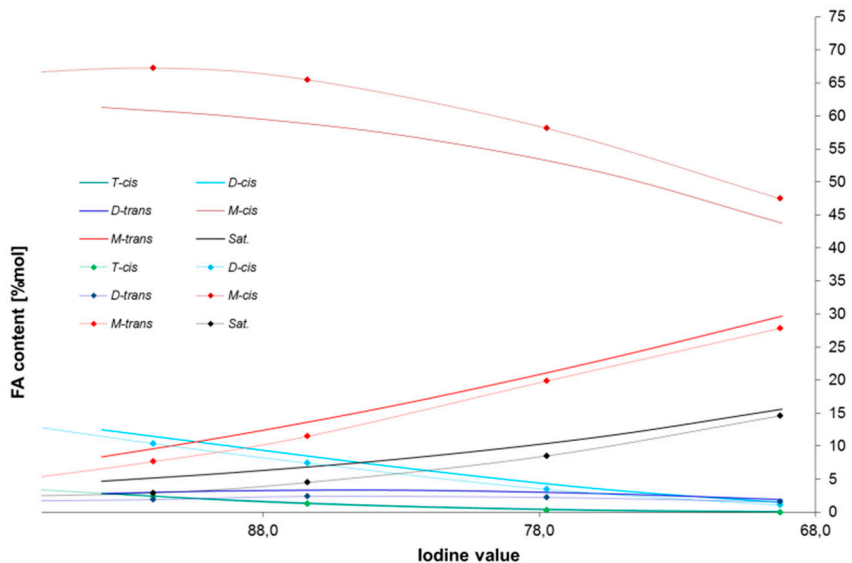


Figure 5. Predicted (solid line) and experimental (dotted line) fatty acids contents of canola oil hydrogenated with INS Ni_C catalyst. Reaction conditions: temperature 180 °C, H₂ pressure = 6 bar(a), agitation 950 rpm.

A very important catalyst feature in the hydrogenation reaction of vegetable oils is the catalyst selectivity. In hydrogenation studies there is a tendency to optimize catalyst properties and process parameters so that the most unsaturated fatty acids are hydrogenated to oleic acid with a minimal increase in the amount of stearic acid. According to the well-known and accepted method [3,28,32] selectivity of the hydrogenation reaction of fats and vegetable oils can be determined from the ratio of the corresponding rate constants of consecutive reaction steps in Scheme 5: linolenic selectivity $S_{12} = k_1/k_2$ (preference for linolenic acid over linoleic acid hydrogenation) and linoleic selectivity $S_{23} = k_2/k_3$ (preference for linoleic acid over oleic acid hydrogenation).

In the oil industry the linoleic selectivity S_{23} is the most important parameter. Moreover, it is known that an increase of pressure results in a decrease of the linoleic selectivity. Table 6 presents the

quantitative data on the influence of the hydrogen pressure on various selectivities. Since both linolenic and linoleic selectivities do not take into account the *cis/trans* isomerization, the specific isomerization index $S_i = (k_2 + k_3)/mk_r$ as proposed by Plourde *et al.* is also given [23]. As can be seen, upon increasing the hydrogen pressure from 1.5 to 21 bar(a) the linolenic selectivity was found to decrease from 2.70 to 1.51, whereas the linoleic selectivity decreased four times from 24.17 to 6.05. These changes indicate suppression of the hydrogenation of linolenic and linoleic acids with the increased pressure. This observation is in agreement with the results of the analysis of the fatty acid profile revealing that with the increased pressure the C18:2*cis* content was found to increase slightly from 0.6 wt% at 2.5 bar(a) to 3.3 wt% at 21 bar(a). Moreover, in line with the results and expectations the content of steric acid C18:0 increased considerably from 13.1 wt% at 2.5 bar(a) to 22.1 wt% at 21 bar(a). On the other hand, the increasing hydrogen pressure has a substantial effect on suppressing the *cis/trans* isomerization. The corresponding S_i index, which is a ratio of the total isomerization activity to the saturation activity of the catalyst, was found to decrease from 14.72 at 2.5 bar(a) to 7.17 at 21 bar(a). It indicates that less *trans* isomers are formed at higher pressures as is also reflected in the analysis of the fatty acid profile of the hydrogenated samples.

Table 6. Effect of hydrogen pressure on selectivities S_{12} , S_{23} and S_i for the INS Ni_C catalyst.

Pressure, bar(a)	S_{12}	S_{23}	S_i
1.5	2.70	24.17	-
2.5	2.44	18.15	14.72
6	1.92	12.14	11.45
11	1.85	9.52	8.58
21	1.51	6.05	7.17

3. Materials and Methods

3.1. Materials

As feedstock, a refined, bleached, low-erucic acid canola oil was used. The nickel catalyst INS Ni_C was prepared from a fine precursor obtained by means of coprecipitation. The precursor is, chemically, a mixture of nickel-aluminum hydroxycarbonates with a general formula: $Ni_mAl_n(CO_3)_x(OH)_y \times zH_2O$. The coprecipitation was carried out from aqueous solutions of nickel nitrate and sodium aluminate of appropriate concentrations using a $Na_2CO_3/NaOH$ mixture as a precipitating agent. The reaction conditions were as follows: temperature $80 \pm 5^\circ C$, pH in the range 7.0–7.4. The resulting precipitate was filtered and washed with deionized water until the conductivity of a filtrate below $300 \mu S$ was achieved. The INS Ni precursor was then dried in a laboratory drier at $105^\circ C$ for 12 h. The composition of the precursor as calculated after calcination was 85.7 wt% NiO and 14.3 wt% Al_2O_3 . The catalyst precursor was then reduced in hydrogen in the temperature range of 450 – $550^\circ C$ for 4 h. After reduction the resulting pyrophoric residue was protected from oxidation by mixing with liquefied hydrogenated soybean oil under ambient atmosphere. Such a mixture was then cooled down in order to solidify. After dilution with the hydrogenated protecting fat the final catalyst INS Ni_C contained 5.64 wt% of nickel.

3.2. Characterization

The chemical composition of precursors was determined by means of the WDXRF method using a Panalytical Axios spectrometer (Panalytical, Almelo, Netherlands). The specific surface area of the samples was determined by means of the nitrogen adsorption method at the temperature of liquid nitrogen ($-196^\circ C$) using a Micromeritics ASAP 2050 analyzer (Micromeritics, Norcross, GA, USA). The BET isotherms were measured in the p/p_0 range 0.05–0.3. The pore volume and pore size distribution (in the pore size range from 2 to 300 nm) were determined from N_2 adsorption isotherm in the $p/p_0 = 0.02$ –0.99 using the BJH method. The nickel surface area (S_{Ni}) was determined

via oxygen chemisorption at the temperature of 0 °C using a Micromeritics AutoChem 2950HP analyzer (Micromeritics, Norcross, GA, USA) and according to the reaction: 2Ni + O₂ → 2NiO. Before the measurement, a sample was reduced with hydrogen at 500 °C for 2 h. The nickel surface area, dispersion, and average nickel crystallite size parameters were calculated from the following equations:

$$S_{\text{Ni}-A} = \frac{n_m \cdot x_{\text{Ni}} \cdot N_A \cdot A_V}{m_p} \quad (4)$$

where:

$S_{\text{Ni}-A}$: nickel surface area per 1 g of catalyst [m²/g_{cat}]

n_m : number of moles of a gas adsorbate used during a measurement [mol]

x_{Ni} : number of moles of a metal corresponding to 1 mol of the gas adsorbate under the measurement conditions (1.1765 mol Ni/mol O₂)

N_A : nickel atom area [m²] (N_A for Ni = 6.45 · 10⁻²⁰ m²)

A_V : Avogadro's number (6.023 × 10²³ at/mol)

m_p : sample weight [g]

$$S_{\text{Ni}-B} = \frac{n_m \cdot x_{\text{Ni}} \cdot N_A \cdot A_V \cdot 100}{\%_{\text{Ni}} \cdot m_p} \quad (5)$$

where:

$S_{\text{Ni}-B}$: nickel surface area per 1 g of nickel [m²/g_{Ni}]

$\%_{\text{Ni}}$: nickel content in a sample [%]

$$D = \frac{n_m \cdot x_{\text{Ni}} \cdot M_{\text{Ni}} \cdot 10^4}{\%_{\text{Ni}} \cdot m_p} \quad (6)$$

where:

D : nickel dispersion [%]

M_{Ni} : molar mass [g/mol]

$$d = \frac{6}{S_{\text{Ni}} \cdot g_{\text{Ni}}} \quad (7)$$

where:

d : average nickel crystallite size [nm]

g_{Ni} : nickel density [kg/dm³]

3.3. Methods

The hydrogenation reactions were carried out on an installation shown in Figure 6. The essential parts of this installation include: pressure batch reactor Parr 5500, pressure, temperature and stirring speed controller, hydrogen reservoir (volume 1.0 × 10⁻⁴ m³), and digital manometer with an accuracy up to 0.1 bar. The tests were performed under the following conditions: temperature 180 °C, constant pressure in the autoclave (1.5, 2.5, 6, 11, and 21 bar(a)), stirring speed 950 rpm, concentration of the INS Ni_C catalyst in oil 0.03 wt% (as Ni), 25 g of canola oil. Hydrogen was supplied to a reaction mixture from the bottom by means of a dip tube. The autoclave was loaded with a suspension of the catalyst in oil, the system was evacuated several times and filled with hydrogen in order to remove oxygen. The suspension was then heated under slight vacuum to the required temperature followed by loading the autoclave with hydrogen to the working pressure. The stirring was started and the reaction time was counted from that moment. In order to maintain the constant pressure during hydrogenation,

the hydrogen consumed in the course of the reaction was continuously supplied from the reservoir. A decrease of hydrogen pressure in the reservoir was a measure of the hydrogen consumption for hydrogenation of canola oil. After the test, the catalyst was filtered off and a liquid fraction was subjected to analysis.

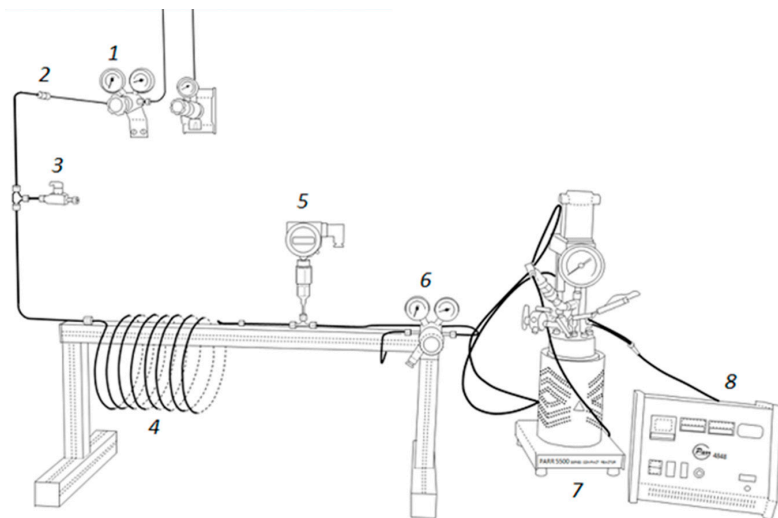


Figure 6. Hydrogenation installation: 1 and 6-pressure reduction valves, 2-stopcock, 3-side valve, 4-hydrogen reservoir, 5-manometer with display, 7-autoclave Parr 5500, 8-pressure, temperature, and stirring speed controller.

The iodine value (IV) was controlled by means of refractometry. The final iodine value was determined by means of a titration method using a Wijs reagent [33]. The FA profiles of hydrogenated samples were analysed by means of gas chromatography coupled with mass spectrometry using a Shimadzu GC-MS2010Ultra instrument (Shimadzu, Kyoto, Japan). The oil samples were subjected to derivatization prior to analysis in order to obtain methyl esters of fatty acids (FAME). A 10 mg sample of hydrogenated canola oil was dissolved in 500 μ L *t*-butylmethylether, 250 μ m 0.1% TMSH in MeOH (Fluka) was added and a mixture was vigorously shaken for 45–60 s. The sample was analyzed using the following conditions: BPX column, 120 m \times 0.25 mm \times 20 μ m, isothermal programme 180 °C for 110 min, helium flow 1.0 mL/min, split 100:1. The peaks of particular FAMEs were identified based on mass spectra by comparison with a FAME Mix standard from Restek (37 components). The content of fatty acids was determined by means of the internal normalization, assuming similar response factors of a FID detector for structurally-similar FAME compounds. Each sample was analyzed three times and the average values from three runs for each FA are presented.

4. Conclusions

The effect of hydrogen pressure on kinetics of the canola oil hydrogenation reaction has been quantitatively described. An increase of values of all rate constants for the corresponding hydrogenation steps was observed with the increasing pressure, with the largest increase being observed for the rate constant of hydrogenation of monoenes to stearic acid. This results in a remarkable decrease of the linoleic selectivity of the nickel catalyst. Moreover, a concurrent decrease of the *cis/trans* monoene isomerization rate was also found that was reflected by a two-fold decrease of the specific isomerization index. The results, thus, provide detailed information to what extent the increasing hydrogen pressure facilitates hydrogenation over *cis/trans* isomerization.

The fatty acid profiles of canola oil samples hydrogenated to the same iodine value using an industrial nickel catalyst were found to depend on the hydrogenation pressure. The content of elaidic acid, 9*t*-C18:1 and other positional isomers decreased by *ca.* 37% with the increasing pressure

from 2.5 to 21 bar(a). This was accompanied by a concurrent increase of the stearic acid content from 13 to 22 wt%. Furthermore, a novel simplified three-step model of the hydrogenation of canola oil over a nickel catalyst proved to be a useful tool to predict the course of the hydrogenation process and concentrations of fatty acids within the iodine value range important from the industrial viewpoint.

Author Contributions: Andrzej Gołębowski suggested and supervised the work. Marcin Konkol wrote the main manuscript with input from all authors and prepared all the schemes, figures and tables. Robert Bicki performed the hydrogenation experiments and GCMS analyses. Waldemar Wróbel performed the calculations of rate constants. All authors reviewed the manuscript.

Conflicts of Interest: The authors declare no conflict of interest.

References

1. Beers, A.; Ariaansz, R.; Okonek, D. Trans isomer control in hydrogenation of edible oils. In *Trans Fatty Acids*; Dijkstra, A.J., Hamilton, R.J., Hamm, W., Eds.; Blackwell Publishing: Oxford, UK, 2008; p. 158.
2. Jang, E.S.; Jung, M.Y.; Min, D.B. Hydrogenation for low trans and high conjugated fatty acids. *Compr. Rev. Food Sci. Food Saf.* **2005**, *1*, 22–30. [[CrossRef](#)]
3. Bartholomew, C.H.; Farrauto, R.J. *Fundamentals of Industrial Catalytic Processes*; John Wiley & Sons Inc.: Hoboken, NJ, USA, 2006; Chapter 7; pp. 524–531.
4. Veldsink, J.W.; Bouma, M.J.; Schöön, N.H.; Beenackers, A.A.C.M. Heterogeneous Hydrogenation of Vegetable Oils: A Literature Review. *Catal. Rev. Sci. Eng.* **1997**, *39*, 253–318. [[CrossRef](#)]
5. Dijkstra, A.J. Revisiting the formation of trans isomers during partial hydrogenation of triacylglycerol oils. *Eur. J. Lipid Sci. Technol.* **2006**, *108*, 249–264. [[CrossRef](#)]
6. Musavi, A.; Cizmeci, M.; Tekin, A.; Kayahan, M. Effects of hydrogenation parameters on trans isomer formation, selectivity and melting properties of fat. *Eur. J. Lipid Sci. Technol.* **2008**, *110*, 254–260. [[CrossRef](#)]
7. Balakos, M.W.; Hernandez, E.E. Catalyst characteristics and performance in edible oil hydrogenation. *Catal. Today* **1997**, *35*, 415–425. [[CrossRef](#)]
8. Cheng, H.N.; Dowd, M.K.; Easson, M.W.; Condon, B.D. Hydrogenation of cottonseed oil with nickel, palladium and platinum catalysts. *J. Am. Oil Chem. Soc.* **2012**, *89*, 1557–1566. [[CrossRef](#)]
9. Hashimoto, K.; Muroyama, K.; Nagata, S. Kinetics of the hydrogenation of fatty oils. *J. Am. Oil. Chem. Soc.* **1971**, *49*, 291–295. [[CrossRef](#)]
10. Fillion, B.; Morsi, B.I.; Heier, K.R.; Machado, R.M. Kinetics, gas-liquid mass transfer, and modeling of the soybean oil hydrogenation process. *Ind. Eng. Chem. Res.* **2002**, *41*, 697–709. [[CrossRef](#)]
11. Eldib, I.A.; Albright, L.F. Operating variables in hydrogenating cottonseed oil. *Ind. Eng. Chem.* **1957**, *49*, 825–831. [[CrossRef](#)]
12. Wisniak, J.; Albright, L.F. Hydrogenating cottonseed oil at relatively high pressure. *Ind. Eng. Chem.* **1961**, *53*, 375–380. [[CrossRef](#)]
13. Marangozis, J.; Keramidas, O.B.; Paparisvas, G. Rate and mechanism of hydrogenation of cottonseed oil in slurry reactors. *Ind. Eng. Chem. Process. Des. Dev.* **1977**, *16*, 361–369. [[CrossRef](#)]
14. Krishnaiah, D.; Sarkar, S. Kinetics of liquid phase hydrogenation of cottonseed oil with nickel catalysts. *J. Am. Oil. Chem. Soc.* **1990**, *67*, 233–238. [[CrossRef](#)]
15. Bailey, A.E. Theory and mechanism of the hydrogenation of edible oil. *J. Am. Oil. Chem. Soc.* **1949**, *26*, 596–601.
16. Bern, L.; Hell, M.; Schöön, N.H. Kinetics of hydrogenation of rapeseed oil. 2. Rate equations of chemical reactions. *J. Am. Oil Chem. Soc.* **1975**, *52*, 391–394. [[CrossRef](#)]
17. Chen, A.H.; McIntire, D.D.; Allen, R.R. Modeling of reaction rate constants and selectivities in soybean oil hydrogenation. *J. Am. Oil Chem. Soc.* **1981**, *58*, 816–818. [[CrossRef](#)]
18. Allen, R.R. Hydrogenation. *J. Am. Oil Chem. Soc.* **1981**, *58*, 166–169. [[CrossRef](#)]
19. Colen, G.C.M.; van Duijn, G.; van Oosten, H.J. Effect of pore diffusion on the triacylglycerol distribution of partially hydrogenated trioleoylglycerol. *Appl. Catal.* **1988**, *43*, 339–350. [[CrossRef](#)]
20. Gut, G.; Kosinka, J.; Prabucki, A.; Schuerch, A. Kinetics of the liquid-phase hydrogenation and isomerization of sunflower seed oil with nickel catalysts. *Chem. Eng. Sci.* **1979**, *34*, 1051–1056. [[CrossRef](#)]
21. Susu, A.A.; Ogunye, A.F. Nickel-catalyzed hydrogenation of soybean oil. 1. Kinetic, equilibrium and mass-transfer determinations. *J. Am. Oil Chem. Soc.* **1981**, *58*, 657–661. [[CrossRef](#)]

22. Susu, A.A. Kinetics, mass-transfer and scale-up in nickel-catalyzed oil hydrogenators. *Appl. Catal.* **1982**, *4*, 307–320. [[CrossRef](#)]
23. Plourde, M.; Belkacemi, K.; Arul, J. Hydrogenation of sunflower oil with novel Pd catalysts supported on structured silica. *Ind. Eng. Chem. Res.* **2004**, *43*, 2382–2390. [[CrossRef](#)]
24. Jovanović, D.; Čupić, Ž.; Stanković, M.; Rožić, L.; Marković, B. The influence of the isomerization reactions on the soybean oil hydrogenation process. *J. Mol. Catal. A* **2000**, *159*, 353–357. [[CrossRef](#)]
25. Cheng, H.N.; Rau, M.W.; Dowd, M.K.; Easson, M.W.; Condon, B.D. Comparison of soybean and cottonseed oils upon hydrogenation with nickel, palladium and platinum catalysts. *J. Am. Oil Chem. Soc.* **2014**, *91*, 1461–1469. [[CrossRef](#)]
26. Holser, R.A.; List, G.R.; King, J.W.; Holliday, R.L.; Neff, W.E. Modeling of hydrogenation kinetics from triglyceride compositional data. *J. Agric. Food Chem.* **2002**, *50*, 7111–7113. [[CrossRef](#)] [[PubMed](#)]
27. List, G.R.; Neff, W.E.; Holliday, R.L.; King, J.W.; Holser, R. Hydrogenation of soybean oil triglycerides: Effect of pressure on selectivity. *J. Am. Oil Chem. Soc.* **2000**, *77*, 311–314. [[CrossRef](#)]
28. Coenen, J.W.E. Catalytic hydrogenation of fatty oils. *Ind. Eng. Chem. Fundam.* **1986**, *25*, 43–52. [[CrossRef](#)]
29. Andersson, K.; Hell, M.; Löwendahl, L.; Schöön, N.H. Diffusivities of hydrogen and glyceryl trioleate in cottonseed oil at elevated temperature. *J. Am. Oil Chem. Soc.* **1974**, *51*, 171–173. [[CrossRef](#)]
30. Horiuti, I.; Polanyi, M. Exchange reactions of hydrogen on metallic catalysts. *Trans. Faraday Soc.* **1934**, *30*, 1164–1172. [[CrossRef](#)]
31. Lidefelt, J.O.; Magnusson, J.; Schöön, N.H. The role of hydrogen in the selectivity of vapor-phase hydrogenation of methyl linoleate. *J. Am. Oil Chem. Soc.* **1983**, *60*, 608–613. [[CrossRef](#)]
32. Albright, L.F. Quantitative measure of selectivity of hydrogenation of triglycerides. *J. Am. Oil Chem. Soc.* **1965**, *42*, 250–253. [[CrossRef](#)]
33. Method PN-EN ISO 3961. Available online: <http://sklep.pkn.pl/pn-en-iso-3961-2013-10e.html> (accessed on 1 April 2016).



© 2016 by the authors; licensee MDPI, Basel, Switzerland. This article is an open access article distributed under the terms and conditions of the Creative Commons by Attribution (CC-BY) license (<http://creativecommons.org/licenses/by/4.0/>).